Metal to Insulator Transition in Films of Molecularly Linked Gold Nanoparticles

Amir Zabet-Khosousi,* Paul-Emile Trudeau,* Yoshinori Suganuma, and Al-Amin Dhirani*,†
Department of Chemistry, University of Toronto, Toronto, Ontario, M5S 3H6, Canada

Bryan Statt
Department of Physics, University of Toronto, Toronto, Ontario, M5S 1A7, Canada
(Received 30 August 2004; revised manuscript received 17 February 2006; published 21 April 2006)

We report a metal to insulator transition (MIT) in disordered films of molecularly linked gold nanoparticles (NPs). As the number of carbons (n) of alkanedithiol linker molecules (C_nS_2) is varied, resistance (R) at low temperature ($T = 2$ K) and at 200 K, as well as trends in R vs T data at intermediate temperatures, all point to an MIT occurring at $n = 5$. We describe these results in a context of a Mott-Hubbard MIT. We find that all insulating samples ($n \geq 5$) exhibit a universal scaling behavior $R \sim \exp[(T_0/T)^{\nu}]$ with $\nu = 0.65$, and all metallic samples ($n \leq 5$) exhibit weaker R-T dependencies than bulk gold. We discuss these observations in terms of competitive thermally activated processes and strong, T-independent elastic scattering, respectively.

DOI: 10.1103/PhysRevLett.96.156403 PACS numbers: 71.30.+h, 05.60.Gg, 81.07.Pr

Mott-Hubbard and Anderson localization models form the foundation of much of our microscopic understanding of metal-insulation transitions (MITs) [1]. The former is based on a lattice of atoms with electrons that interact via on-site repulsion and intersite transfer. As intersite transfer increases, initially localized electrons can become itinerant, resulting in an MIT. Mott's original model envisioned driving the transition by changing interatomic spacing. In the other extreme of noninteracting electrons, Anderson showed that sufficiently large fluctuations in electrostatic potential, induced by defects, can cause initially itinerant electrons to become localized.

Nanoparticle (NP) superlattices or "artificial materials"—a novel class of materials comprising assemblies of NPs ("artificial atoms") and molecules—provide a new controlled platform for exploring MIT [2]. Advances in NP synthesis permit control over chemical composition and size distribution, in turn impacting NPs charging energies and superlattice disorder [3]. Also, couplings can be controlled via inter-NP spacing and structure of molecular backbones and capping groups [4]. An attractive prototype molecular system is alkanedithiols [$HS(CH_2)_nSH$ or C_nS_2] since their properties have been extensively studied; they can bind to Au via the thiol (-SH) groups; and they offer control over average spacing between linked NPs via choice of n [5]. For sufficiently large n, electrical conductivity of the alkane chain is determined by tunneling and varies exponentially with n [6,7].

Self-assembled films of C_nS_2-linked Au NPs exhibit electrical behaviors that range from insulating [8] to metallic-like [9]. Observation of these limits, combined with a possibility of varying average inter-NP separation 1 C-C bond at a time, raises an intriguing prospect of exploring a Mott-Hubbard MIT in these systems along lines originally envisioned by Mott. Studies of systematically compressed monothiol-capped NP films formed using Langmuir-Blodgett methods point to this possibility [2]. Density of states measurements by scanning tunneling microscopy as well as optical measurements of these films provide evidence of strong quantum coupling or exchange interaction between NPs [10]. However, attempts to observe MIT using highly compressed Ag NP arrays have been hampered by defects including domain boundaries in 2D and a need for narrow (~3%) size distributions [3].

Self-assembled structures prepared using dithiol cross-linkers, although disordered, circumvent the above challenges by forming larger clusters of linked NPs as more material is added, until there is at least one sample-spanning linked pathway at the percolation threshold [9]. In a previous study performed in our lab, a percolation-driven MIT was observed in films of C_4S_2-linked Au NPs [9]. Here we describe results obtained by systematically varying the length of linker molecules from 0.5 nm (C_2S_2) to 1.6 nm ($C_{10}S_2$), in increments of ~0.1 nm (one CH_2 group). Measurements of resistances (R) at both 2 K and 200 K, variation of R with temperature (T) at intermediate T, and changes in R after annealing, all point to a Mott-Hubbard MIT occurring at $n = 5$.

Au NPs 5.0 ± 0.8 nm in diameter, stabilized by tetraoctylammonium bromide (TOAB), were synthesized in toluene [11] and characterized by absorption spectroscopy and transmission electron microscopy. Alkanedithiols (C_nS_2, $n = 2, \ldots, 6, 8, 9, 10$) were purchased. To facilitate overcoming percolation thresholds, films were grown on closely spaced Au electrodes fabricated on glass slides using an electromigration technique [12]. NP films were formed by first functionalizing the Au electrodes by immersing slides in 0.5 mM ethanolic solutions of C_nS_2 for 1 h and rinsing. Next, slides were alternately immersed in toluene solutions of Au NPs for ~30–60 min, and 0.5 mM of dithiols for 10 min with intervening rinse steps. After dithiol immersion and toluene rinse steps, slides were dried

under a gentle flow of nitrogen gas, and R of samples were measured at room temperature using a digital multimeter. When it was necessary to store samples, they were kept under argon and refrigerated. Magnet wires were attached to Au electrodes using indium solder far from the junctions and using minimal heating to avoid damaging the films. R values measured after addition of indium dropped only for some samples with $n = 4$ and 5. Current (I) through the sample as a function of applied voltage (V) at different temperatures ($2\ \mathrm{K} < T < 200\ \mathrm{K}$) was measured using a homemade I-V converter and a liquid Helium cryostat. R values were obtained by fitting straight lines to I-V curves near 0 V. To test reproducibility, at least 4 identically prepared samples for each n were studied. All but 3 samples of 46 studied exhibited stable electrical characteristics as a function of T below 200 K.

Figure 1 shows changes in conductance of typical samples vs number of NP/C_nS_2 exposure cycles. The conductances generally increase after each cycle. Previous optical measurements have shown that film thickness increases in proportion to the number of cycles [13]. A resulting growth of linked-NPs clusters accounts for the increase in the conductance. For $n = 2$ and 3, as the number of cycles increases, conductances change initially very slowly, then rapidly and finally at a constant rate. These observations suggest that a percolation transition occurs, and eventually in the bulk limit, number of current pathways increases in proportion to the average thickness of the film. As n increases, the region of rapid change seems to occur at lower number of cycles, until for $n \geq 5$ this region is no longer observed. For large n, conductance varies nonuniformly with the number of cycles. Similar behavior has been reported in films of hexanethiol-capped NPs linked by C_nS_2 ($n \geq 6$) [14]. Variation in rates of increase may be due to changes in orientation and conformation of alkanedithiols on NPs surfaces [14].

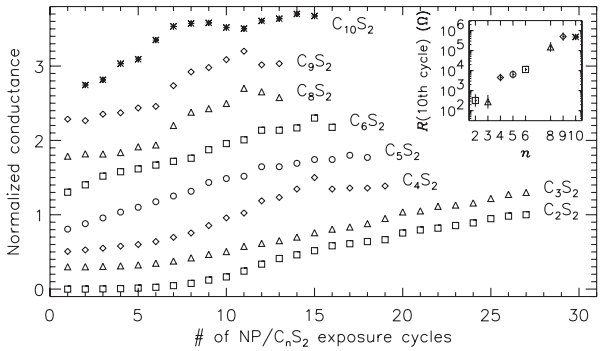

FIG. 1. Normalized conductance of typical samples as a function of number of NP/C_nS_2 exposure cycles for various n. Conductances are normalized with respect to their maximum values. Offsets are added for clarity. Inset: R of the samples after the 10th cycle as a function of n. R was measured before adding indium contacts onto the films on Au electrodes.

Figure 2 shows R of samples with various n, normalized to their values at 200 K, vs T. At low T, two distinct types of behavior are observed: samples with $n \leq 4$ exhibit finite R and are *metallic*; samples with $n \geq 6$ exhibit rapidly increasing R and are *insulating*. Both type of behaviors are observed among samples with $n = 5$. At intermediate T, temperature coefficient of resistance ($\mathrm{TCR} \equiv d(R/R_{200\,\mathrm{K}})/dT$) provides another means to compare behavior of samples. Metals and insulators are known generally to exhibit positive and negative TCR, respectively. This trend is followed by samples with $n \leq 4$ and $n \geq 6$, respectively. For $n = 5$, samples with finite R at low T exhibit positive TCR, except one which is indicated by an arrow, and samples with rapidly increasing R at low T exhibit negative TCR. The inset shows R of the samples at 200 K as a function of n. As the linker length increases from C_2S_2 to C_5S_2, R changes by less than an order of magnitude for metallic samples. Going from insulating to metallic samples with $n = 5$, R jumps by 2 orders. Thereafter, R changes by another $\sim$2 orders for insulating samples ($n \geq 5$). This change can be attributed to the exponential growth of tunneling resistances with distance [$R \sim \exp(\beta n)$ where β is a constant]. The observed β is $\sim$0.9, in agreement with a reported value of 1.0 ± 0.1 for alkanedithiols in single-molecule junctions [6]. We note that the data are highly reproducible: All 12 samples with $n \leq 4$ and 22 samples with $n \geq 6$ show metallic and insulating behavior, respectively. Of 12 samples with $n = 5$, 7 showed metallic and 5 showed insulating behaviors.

According to Mott's model, onset of metallic behavior in a lattice of compressed hydrogen atoms is expected to occur at an interatomic distance of $\sim 4.5a_0$, where a_0 is the Bohr radius. Viewing NPs as artificial atoms, overlap between NPs' wave function should become sufficiently strong at sufficiently small inter-NP separations, and delocalized states should appear [15]. To estimate the critical NP separation, the wave function decay constant $\kappa \approx \sqrt{2m^*\phi}/\hbar$ provides a useful length scale ($a_0 \sim 1/\kappa$), with m^* being the effective mass, ϕ the barrier height,

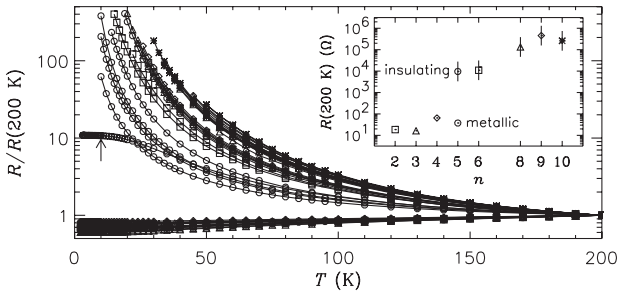

FIG. 2. Normalized R of 43 samples with various n vs T. R's are normalized to their respective values at 200 K. Inset: R of the samples at 200 K as a function of n. R was measured after adding indium contacts onto the films on Au electrodes. The number of exposure cycles for a given n is equal to the maximum shown in Fig. 1.

and $\hbar$ Planck's constant. Taking $\phi \sim 1.4$ eV and $m^* \sim 0.4 \times$ mass of electron for Au-C_nS_2 barriers [16], we find $\kappa \sim 4$ nm^{-1}. Applying Mott's condition for the MIT, we get $4.5/\kappa \sim 1.1$ nm, consistent with inter-NP separation given by C_5S_2 linkers [5].

To test whether observed metallic behavior is a result of Mott-MIT rather than of direct metal-metal contacts between NPs, we annealed our samples under nitrogen atmosphere. The annealed samples initially followed trends in R shown in Fig. 2. Eventually, samples with $n \leq 5$ showed sudden drops of 30–50% in R at $100 \pm 20\,^{\circ}$C. Our results are in agreement with a study showing that, using mass spectroscopy and electron microscopy, annealing releases dithiols, which in turn induces metal-metal contacts between NPs and drops in R [11]. This suggests that before annealing alkanedithiols indeed protect Au NPs from aggregation and point to a Mott mechanism of metallic behavior observed.

The observation of both metallic and insulating behaviors among $n = 5$ samples suggests that other parameters besides n can influence the MIT. Examples include distributions in NP sizes and inter-NP separations for a given n (likely due to presence of solvent or TOAB, or orientation of linkers), and fluctuations in electrostatic potentials due to trapped charges.

Detailed examinations of R-T data show that all insulating samples exhibit a universal behavior [Fig. 3(a)]:

$$R = R_0 \exp[(T_0/T)^{\nu}] \tag{1}$$

where R_0, T_0, and ν are fitting parameters. The upper inset shows that T_0 increases with n implying, as discussed below, an increase in activation energy with increasing inter-NP separation. A lower inset indicates that $\nu = 0.65$. Previous studies of transport mechanisms through insulating NP films have typically found two major types of T dependencies: $\nu = 1$ and $\nu = 1/2$. The fact that we observe a power that lies between these two values suggests that a combination of both mechanisms are operating. To examine this in more detail, we analyzed $\ln(R)$ vs T^{-1} and $T^{-1/2}$ for all insulating samples; Fig. 3(b) shows behavior of a typical sample. Below $\sim$100 K, $\ln(R)$ tends to $T^{-1/2}$ and at higher T to T^{-1} (Arrhenius) behavior. Insets show slopes of best fit lines to T^{-1} and $T^{-1/2}$ behavior for various n. T_0 [Fig. 3(a), inset] and best fit slopes [Fig. 3(b), insets] exhibit similar trends.

Arrhenius behavior can arise from single-electron charging of NPs [5]: $R \sim \exp(E_a/kT) \approx \exp(E_c/kT)$ where E_c is the charging energy of a NP ($E_c = e^2/2C$, with e being the charge of electron, and C the total capacitance of the NP) and k is Boltzmann's constant. Table I lists activation energies (E_a) extracted from the slopes of T^{-1} fits. E_a increases with n, implying that C decreases correspondingly. As the inter-NP separation (s) increases, the contribution of neighboring NPs to C decreases. E_c of a NP with radius r in a granular film can be estimated by an electrostatic model developed by Abeles *et al.* [18]: $E_c = \frac{e^2}{8\pi\epsilon\epsilon_0} \times (\frac{1}{r} - \frac{1}{r+s})$. Taking $\epsilon = 2.6$ and $s = 1.6$ nm for $C_{10}S_2$, we get $E_c \sim 44$ meV which is of the same order as the values observed. The model predicts an increase in E_a with s, as observed.

A $T^{-1/2}$ behavior is predicted for disordered materials by a variable range hopping model (VRH). VRH, introduced by Mott [19] and extended by Efros-Shklovskii (ES) [20] to accommodate strong Coulomb interactions, is based on an interplay between tunneling and activated

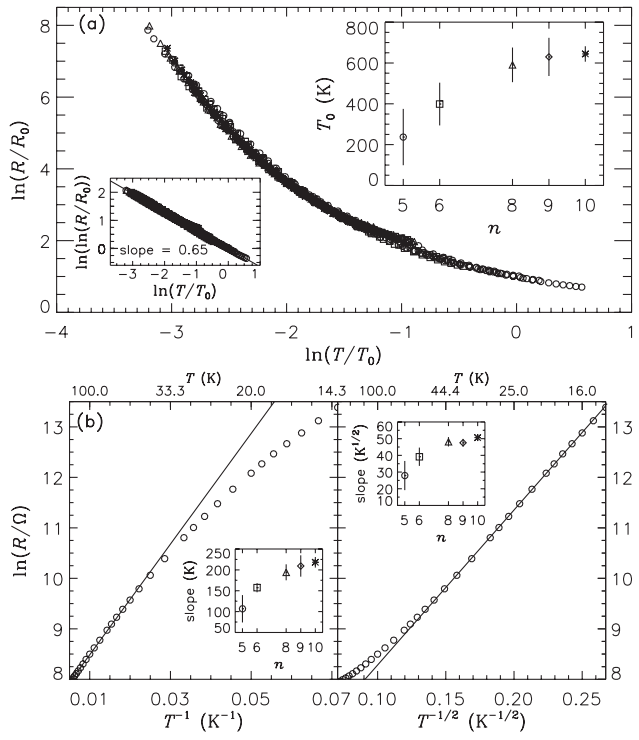

FIG. 3. (a) $\ln(R/R_0)$ vs $\ln(T/T_0)$ for all insulating samples ($n \geq 5$). R_0 and T_0 are fitting parameters. 678 points are overlaid. Upper Inset: Variation of T_0 with n. Lower Inset: $\ln(\ln(R/R_0))$ vs $\ln(T/T_0)$ shows linear behavior. The best fit slope is 0.65. (b) R of a typical insulating sample with $n = 5$ plotted vs T^{-1} and $T^{-1/2}$. Solid lines represent best linear fits for respective data. Insets: Slopes of the linear fits vs n.

TABLE I. Fit parameters for insulating samples obtained from T^{-1} and $T^{-1/2}$ fits, using Arrhenius and VRH models, respectively. Hopping distances (ξ) at 20 K are calculated using the formula $\xi = e^2/(\pi\epsilon\epsilon_0 k\sqrt{TT_{0,\mathrm{VRH}}})$ [17] taking $\epsilon = 2.6$.

n	E_a (meV)	$T_{0,\mathrm{VRH}}$ (K)	$\xi_{20\,\mathrm{K}}$ (nm)
5	9.2	780	207
6	13.6	1534	147
8	16.7	2317	120
9	18.1	2260	121
10	18.8	2564	114

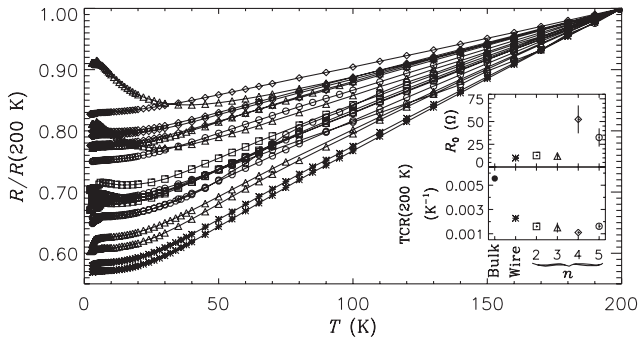

FIG. 4. R of metallic samples ($n \leq 5$) and thin gold wires normalized to their values at 200 K vs T. Upper Inset: Residual resistance of metallic samples extrapolated as $T \rightarrow 0$ vs type of samples. Lower Inset: TCR of the metallic samples at 200 K vs type of samples. The same symbols are used to represent sample-types in both insets (see abscissa) and main panel.

processes. Although the ES-VRH model predicts the $T^{-1/2}$ behavior observed in linked-NP films [21], its applicability to these systems is not clear [17,22]. For example, significant discrepancies between hopping distances (ξ) and tunneling length scales have been observed in linked-NP films [17,22]. ξ for our samples at 20 K extracted using the ES-VRH model are listed in Table I. Observed ξ's are much larger than tunneling distances which are expected to be on the order of 1 nm. Note that ξ is even larger at lower T. Therefore, modifications to the existing model are necessary. We have proposed a ''quasilocalized'' model near the MIT [17], and further efforts exploring $T^{-1/2}$ behavior are ongoing in our lab.

Figure 4 shows normalized R vs T for metallic C_nS_2-linked NP films ($n \leq 5$) and thermally deposited 15 nm thick gold wires. Above 100 K, R varies linearly with T. TCR values, obtained by fitting straight lines to the data above 100 K, are shown in a lower inset. For comparison a value of bulk gold is also shown. TCR of the NP films do not exhibit a systematic trend with n. However, they are lower than the TCR of bulk gold by more than a factor of 2. Assuming a mean free path (l) of 5 nm for electrons in NPs and a Fermi velocity (v_f) of 1.4×10^6 m/s for Au, we estimate an elastic scattering time of $\tau_e \sim l/v_f \approx 3.6$ fs, and an inelastic scattering time of $\tau_i \sim \hbar/kT \approx 38$ fs at 200 K. T-independent elastic scattering dominates the resistance of our samples [23]. Lack of a systematic trend in TCR vs n likely arises due to film disorder. Below 10 K, R for these metallic samples vary slowly (less than 1%) and tend to finite values as T decreases (upper inset) [24]. The tendency of R toward a finite value at very low T indicates that these films are fundamentally metallic. Some samples exhibit an increase of R below 50 K. Conductance vs V data of these samples show suppressions at 0 V, which can be attributed to charging effects [25]. However, in these cases as well R stays finite as T becomes small.

In conclusion, our data provide strong evidence for a Mott MIT in films of C_nS_2-linked Au NPs at $n = 5$. These results highlight that such novel materials can exhibit a wide range of electronic properties controllable via nanoscale architecture and serve as a new platform for exploring fundamental charge transport phenomena.

We acknowledge the Natural Science and Engineering Research Council of Canada for support, J. L. Dunford for producing Au NPs, and the R. Birgeneau group for use of the liquid Helium cryostat.

*Corresponding author.
†Electronic address: adhirani@chem.utoronto.ca

[1] N. F. Mott, Proc. R. Soc. A **382**, 1 (1982); P. W. Anderson, Phys. Rev. **109**, 1492 (1958); E. Chacón, J. P. Hernandez, and P. Tarazona, Phys. Rev. B **52**, 9330 (1995).
[2] C. P. Collier, T. Vossmeyer, and J. R. Heath, Annu. Rev. Phys. Chem. **49**, 371 (1998).
[3] K. C. Beverly, J. F. Sampaio, and J. R. Heath, J. Phys. Chem. B **106**, 2131 (2002).
[4] R. H. Terril *et al.*, J. Am. Chem. Soc. **117**, 12 537 (1995); M. D. Musick *et al.*, Chem. Mater. **12**, 2869 (2000); M. Brust and C. J. Keily, Colloids Surf. A **202**, 175 (2002).
[5] M. Brust *et al.*, Adv. Mater. **7**, 795 (1995).
[6] B. Xu and N. J. Tao, Science **301**, 1221 (2003).
[7] C. Kaun and H. Guo, Nano Lett. **3**, 1521 (2003).
[8] J. M. Wessels *et al.*, J. Am. Chem. Soc. **126**, 3349 (2004).
[9] P.-E. Trudeau *et al.*, J. Chem. Phys. **117**, 3978 (2002).
[10] G. Markovich, C. P. Collier, and J. R. Heath, Phys. Rev. Lett. **80**, 3807 (1998); G. Medeiros-Ribeiro *et al.*, Phys. Rev. B **59**, 1633 (1999).
[11] N. Fishelson *et al.*, Langmuir **17**, 403 (2001).
[12] A. Zabet-Khosousi *et al.*, Phys. Rev. Lett. **94**, 096801 (2005); H. Park *et al.*, Appl. Phys. Lett. **75**, 301 (1999).
[13] M. Brust *et al.*, Langmuir **14**, 5425 (1998).
[14] A. W. Snow *et al.*, J. Mater. Chem. **12**, 1222 (2002).
[15] C. A. Stafford and S. Das Sarma, Phys. Rev. Lett. **72**, 3590 (1994).
[16] W. Wang, T. Lee, and M. A. Reed, J. Phys. Chem. B **108**, 18 398 (2004).
[17] J. L. Dunford *et al.*, Phys. Rev. B **72**, 075441 (2005).
[18] B. Abeles, P. Sheng, M. D. Coutts, and Y. Arie, Adv. Phys. **24**, 407 (1975).
[19] N. F. Mott, J. Non-Cryst. Solids **1**, 1 (1968).
[20] B. I. Shklovskii and A. L. Efros, *Electronic Properties of Doped Semiconductors* (Springer, New York, 1984).
[21] D. Yu *et al.*, Phys. Rev. Lett. **92**, 216802 (2004).
[22] T. B. Tran *et al.*, Phys. Rev. Lett. **95**, 076806 (2005).
[23] T. J. Coutts, *Electrical Conduction in Thin Metal Films* (Elsevier, Amsterdam, 1974).
[24] Below 6 K, some samples show a sudden drop in R, which is probably due to superconductivity of indium contacts. The drop in R is $\sim 0.3\ \Omega$ which is in agreement with estimated contact resistances of indium solders.
[25] P.-E. Trudeau, A. Escorcia, and A.-A. Dhirani, J. Chem. Phys. **119**, 5267 (2003).